The dynamic polarization potential and dynamical non-locality in nuclear potentials: Deuteron-nucleus potential

R. S. Mackintosh*

School of Physical Sciences, The Open University, Milton Keynes, MK7 6AA, UK

N. Keeley†

National Centre for Nuclear Research,

ul Andrzeja Sołtana 7, 05-400 Otwock, Poland

(Dated: October 25, 2016)

arXiv:1610.07378v1 [nucl-th] 24 Oct 2016

Abstract

The consequences for direct reactions of the dynamical non-locality generated by the excitation of the target and projectile are much less studied than the effects of non-locality arising from exchange processes. Here we are concerned with the dynamical non-locality due to projectile excitation in deuteron induced reactions. The consequences of this non-locality can be studied by the comparison of deuteron induced direct reactions calculated with alternative representations of the elastic channel wave functions: (i) the elastic channel wave functions from coupled channel (CC) calculations involving specific reaction processes, and, (ii) elastic channel wave functions calculated from local potentials that exactly reproduce the elastic scattering S-matrix from the same CC calculations. In this work we produce the local equivalent deuteron potentials required for the study of direct reactions involving deuterons. These will enable the study of the effects of dynamical non-locality following a method previously employed in an investigation of the effects of non-locality due to target excitation. In this work we consider only excitations due to deuteron breakup, and some new properties of the breakup dynamical polarization potential (DPP) emerge that reveal dynamical non-locality directly. In addition, we evaluate the TELP inversion method and find that it fails to reproduce some features of the DPP due to breakup.

PACS numbers: 24.10.-i, 24.50.+g, 25.45.Ht, 25.45.De

*Electronic address: raymond.mackintosh@open.ac.uk

†Electronic address: nicholas.keeley@ncbj.gov.pl

I. INTRODUCTION

Dynamical non-locality is present in nucleus-nucleus interactions as a result of coupling between the elastic channel and inelastic and reaction channels. It is a property of the non-local dynamical polarization potential, DPP, that is generated by the coupling [1]. It is much less studied than exchange non-locality and its effects are not generally accounted for in the DWBA analysis of direct reactions. The inclusion of dynamical non-locality in DWBA calculations is not amenable to relatively simple corrections that are applied to exchange non-locality. This and other aspects of dynamical non-locality are discussed in Ref. [2] which introduces a method for including it in direct reaction calculations without requiring the solution of integro-differential equations. The method was used to study the dynamical non-locality of the nucleon optical potential that arises from coupling to collective states of the target nucleus. This was accomplished by comparing angular distributions for nucleon transfer reactions involving two alternative representations of the nucleon optical model potential, OMP. The alternative nucleon potentials were: (i) a potential having dynamically induced non-locality, and, (ii) a local potential having an identical partial wave S-matrix S_l (and hence identical elastic scattering observables) for all values of the partial wave orbital angular momentum l. The local potential was derived from the S-matrix of the non-local potential by $S_l \rightarrow V(r)$ inversion. The details are in Ref. [2].

The same general approach can be applied to the study of the non-locality arising from the excitation of a projectile rather than the target. The case of deuteron scattering is of particular interest since, of all nuclei, its cluster structure is best understood. Moreover, deuteron induced reactions are a very important source of spectroscopic information. In a subsequent paper we will study the effect of dynamically induced non-locality in various deuteron induced reactions: (d,t), (d,p) and $(d,{}^6\mathrm{Li})$. The dynamical non-locality is generated by coupling to breakup states as the deuteron interacts with a target nucleus. The consequences of this non-locality can then be evaluated by comparing angular distributions for (d,p), and other deuteron-induced reactions, calculated (i) with dynamically non-local deuteron OMPs, and (ii) with their local equivalents. The local deuteron OMPs have the same S-matrix and hence elastic scattering observables as the dynamically non-local OMPs. This procedure will not incorporate the complete effects of deuteron breakup in (d,p) reactions, see Ref. [3, 4], just the effect of the dynamical non-locality that would be relevant

to any direct reaction involving deuterons, (d,t) and $(d,{}^6\mathrm{Li})$ for example. Rather complete descriptions of breakup and exchange processes specifically for (d,p) and (p,d) reactions exist [5]. However, the emphasis in this work is different, being a general study of dynamical non-locality arising from projectile excitations, based on deuterons as a projectile. The effects of this dynamical non-locality on a range of transfer reactions can then be studied applying the procedure of Ref. [2].

Studying the effect of the dynamical non-locality induced by deuteron breakup is motivated in part by the fact that non-locality due to other inelastic processes gives rise to effects on the projectile wave function that are very different from the standard Perey effect. These effects were studied in Ref. [6] and Ref. [7]. The first of these found an 'anti-Perey' effect in a case of rotational coupling, and the more systematic study in the latter defined a 'generalised Perey factor', GPF. In a case where the standard Perey factor would be a uniform 0.85 within the nucleus, this was found to be just the case for Perey-Buck non locality. However, for the case of inelastic scattering involving the excitation of vibrational states of the target, the GPF exhibited a complex pattern of regions where it was greater and less than unity. The GPF being > 1 corresponds to an 'anti-Perey' effect. Effects of this kind are likely to modify the wave function of any projectile involved in a direct reaction. This could therefore make a significant difference for any direct reaction involving that projectile. For this reason the generalised 'Perey' effects due to projectile breakup should be tested directly by means of (d,t), $(d,{}^4\mathrm{He})$, (d,p), $(d,n)$and (d,d'), etc. reactions.

The non-local DPP that is generated by channel coupling is also l-dependent, having a different function of two radial coordinates for each l. However, since l-dependence and non-locality are hard to disentangle, we generally refer just to 'non-locality'. The non-local potentials generated by channel coupling are hard to interpret [8] and the calculation of scattering observable from them requires the solution of integro-differential equations. Simple recipes, like the introduction of a Perey factor, are not available, motivating the procedure presented in Ref. [2]. In that work, the projectile wave function is not calculated from a non-local potential but calculated *in situ*, as it is generated by coupling, using the coupled channel code FRESCO [9]. We follow the same general procedure for non-locality due to projectile excitation.

In this first paper, we present the breakup calculations from which we determine the local equivalent potentials and the corresponding DPPs. These local equivalent potentials

give exactly the same elastic scattering S-matrix, S_l, and hence exactly the same elastic scattering angular distributions, as those resulting when deuteron breakup channels are coupled to the elastic channel. These potentials are determined by exact inversion of the elastic scattering S-matrix, S_l, from specific breakup calculations. We demonstrate that the breakup calculations presented here already provide evidence for dynamical non-locality in deuteron-nucleus scattering.

In a subsequent paper [10] we determine the angular distributions from a range of direct reactions all calculated with dynamical non-locality in the deuteron channel. To evaluate the effect of dynamical non-locality, these angular distributions will be compared with angular distributions calculated using the local deuteron potentials that are determined in the present paper. In this work it has been possible to exploit the calculations presented here to go beyond supporting the evaluation of dynamical non-locality in the subsequent paper. Section II details the deuteron breakup calculations and the inversion leading to local DPPs; Section III presents the DPPs for various classes of breakup and discusses their various generic properties; Section IV presents further implications including direct evidence of non-local effects; Section V evaluates and also exploits the trivially equivalent local potential, TELP, inversion method; Section VI is a general discussion of our findings and the Appendix formally supports an argument in Section IV concerning implications of non-locality.

Throughout this work we use l for partial wave orbital angular momentum and L for the relative orbital angular momentum of the nucleons in a deuteron. Spin is not included in the present calculations.

II. BREAKUP CONTRIBUTIONS TO DEUTERON-NUCLEUS INTERACTIONS

The interaction of a deuteron with a nucleus is strongly modified by the breakup of the deuteron. The coupled discretized continuum channel, CDCC, method for calculating breakup is now well established [11–15]. Although CDCC is not rigorous, it is reasonable for the purpose of the present study.

To study the importance of this dynamical non-locality, we require the local deuteron potential that is S-matrix equivalent to the non-local potential generated by coupling to the breakup states of the deuteron. Such breakup states implicitly contribute [16] to the empirical local deuteron OMP; for a recent study see Ref. [17]. The local deuteron potential,

that we call 'S-matrix equivalent', is determined by $S_l \rightarrow V(r)$ inversion to have exactly the same S-matrix as the elastic channel S-matrix from the CDCC breakup calculations. A local and l-independent representation of the dynamic polarisation potential (DPP) is found by subtracting the elastic channel potential of the breakup calculation (the 'bare' potential) from the potential found by inversion.

A. The deuteron breakup calculations

In the subsequent paper, Ref. [10], we study direct transfer reactions involving 30 MeV deuterons incident upon ^{16}O and we present here the relevant CDCC breakup calculations. These calculations were carried out with the coupled channel code FRESCO [9] which is also used in the transfer calculations with dynamically non-local interactions [10]. The deuteron and its constituent nucleons were all considered to be spinless for the sake of simplicity. The neutron-proton binding potential was of Gaussian form and was taken from Ref. [11]. Coupled discretized continuum channels (CDCC) calculations, similar to those described in Ref. [18], were performed, the n+^{16}O and p+^{16}O optical potentials required as input to the Watanabe-type folding potentials being taken from the global parameterization of Ref. [19]. The $n+p$ continuum was divided up into bins in momentum (k) space of width $\Delta k = 0.1$ fm^{-1} up to a maximum value $k_{\max} = 0.7$ fm^{-1}. Five sets of CDCC calculations were performed, labeled L0, L2, L02, L0andL2 and L024, respectively. These denote calculations with $n+p$ continua of relative angular momentum $L = 0$ only, $L = 2$ only, $L = 0$ and $L = 2$ with full continuum-continuum coupling, $L = 0$ and $L = 2$ with separate couplings between bins with $L = 0$ and bins with $L = 2$ only (i.e. no couplings between bins with $L = 0$ and $L = 2$), and $L = 0$, $L = 2$ and $L = 4$ with full continuum-continuum coupling, respectively. Comparison of the inverted potentials from certain combinations of these cases will reveal direct evidence of effective non-locality in deuteron-nucleus interactions. We also present the characteristics of DPPs calculated in similar calculations which show that the general properties are generic.

B. The S-matrix inversion

The S-matrix inversion is carried out using the iterative-perturbative, IP, algorithm [16, 20–23] applied to the elastic channel S_l from the deuteron breakup calculation. The IP method provides a local potential yielding S-matrix elements that are effectively indistinguishable from those of the non-local potential, and hence leading to indistinguishable scattering observables. In some cases, the potentials found by inversion have a degree of undulatory behavior in the surface which becomes more pronounced as the S-matrix S_l from the inverted potential more closely approaches S_l for the non-local potential. A strongly undulatory character is characteristic of potentials determined by fitting the S-matrix S_l calculated from potentials that are known to be l-dependent. In fact, potentials found by inverting S_l resulting from the many coupled channels calculations that have been studied *always* have some degree of well-established undulatory character; DPPs are never smooth and certainly never proportional to the bare potential. All the inverted potentials discussed herein have that property. IP inversion can handle spin-$\frac{1}{2}$ and spin-1 projectiles, but for the present purposes and to simplify the deuteron breakup calculations we ignore nucleon spin throughout. An evaluation of the effects of deuteron non-locality upon the J-dependence and analysing powers of transfer reactions must therefore await a future extension of this work. The sensitivity of the scattering to the DPP at various values of the deuteron-nucleus separation can be established by notch tests.

An alternative method of inversion determines the trivially equivalent local potential, TELP, Ref. [24]. A form of this potential with appropriate partial wave weighting [25] is incorporated in the FRESCO code [9] and it is this weighted TELP (referred to here as just TELP), that is commonly used to derive DPPs. It has been evaluated against exact IP inversion and has been shown to be deficient [26] in specific situations, and further evidence is presented below. IP inversion leads to a potential that will precisely reproduce the elastic scattering angular distribution from the CDCC calculation. Although TELP inversion turns out to be inadequate, in general, as an inversion method, we nevertheless find it useful. With IP inversion, the iterative process can start from any 'starting reference potential', SRP. In studies such as the present, the SRP is often taken to be the bare potential of the coupled channel calculation. The DPP can then be calculated immediately by subtraction. However, when the inverted potential is expected to have some undulatory features, as in the present

case, it is helpful to start the iterative process from a potential that can be presumed to be a closer approximation to the target potential. We therefore carried out inversions using the TELP as the SRP. In most cases, the final converged potential was very close to the potential found using the bare potential as SRP. In some cases, the potential was smoother in the surface, eliminating some spurious undulations in that region. However, the overall undulatory features, extending for deuterons to the nuclear centre, were essentially identical with each SRP. We conclude that TELP potentials are useful as the SRP for IP S-matrix inversion.

As a by-product of the use of TELP as SRP, we were able extract the DPPs as calculated from the TELP, and thus evaluate the use of the TELP for determining DPPs. This evaluation of TELP inversion for the present scattering case is presented in Section V.

III. DEUTERON BREAKUP: DYNAMICAL POLARIZATION POTENTIALS

Inversion of the elastic scattering S-matrix S_l that is generated by breakup coupling, for cases L02 and L024, yields the potentials presented in Fig. 1 where they are compared with the bare potential. These potentials will form the basis of the determination of non-local effects in Ref. [10]. The DPP in each case is found by subtracting the bare potential, and the effect of the coupling is more apparent when these DPPs are plotted. The L02 and L024 DPPs are shown in Fig. 2. The imaginary DPPs have emissive regions, more significantly in the L024 case. These properties can be considered well established and notch tests reveal that a peak in the sensitivity occurs for a notch at around 2 fm, with considerable sensitivity down to 1 fm and less. The significant oscillatory features apparent in Fig. 1 and Fig. 2 are therefore well within the radial range to which the elastic scattering angular distribution is sensitive. The emissive features in the DPP do not generally lead to emissivity in the inverted potential. An exception can be seen at around 8 fm in Fig. 1; this cannot lead to $|S_l|$ breaking the unitarity limit and S_l for this potential very closely fits the (unitarity respecting) S_l from the CDCC code. Establishing such undulatary features is not possible with approximate inversion procedures such as the weighted TELP, as we shall show.

In Fig. 3 we compare the DPPs for three cases: L0, L2 and L0andL2, that is for breakup to $L = 0$ states alone, breakup to $L = 2$ states alone and the case when both $L = 0$ continuum states and $L = 2$ continuum states are coupled to the elastic channel, but (unlike the L02

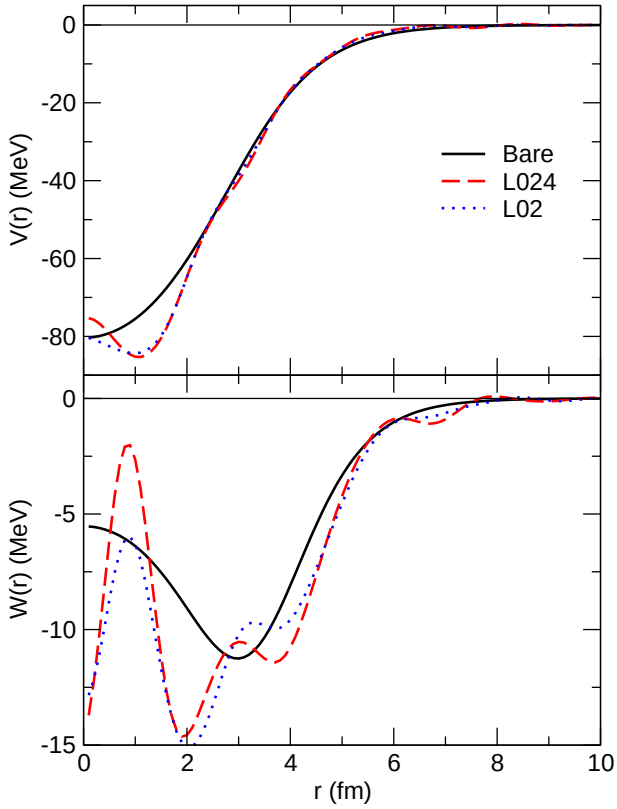

FIG. 1: For 30.0 MeV deuterons on ^{16}O, showing the contribution of specific breakup couplings to the real (top panel) and imaginary (lower panel) elastic scattering interaction. The solid lines are for the bare interaction, the dotted lines are for the potential found by inversion for the L02 coupling case (defined in the text) and the dashed lines show the potential found by inversion for the L024 case.

case) with no mutual coupling between them. The $L = 0$ coupling is overall attractive, while $L = 2$ coupling is overall repulsive, apparently a generic feature, see Ref. [17]. The differences between the L0andL2 and L02 DPPs, that are apparent from a comparison of the solid lines in Fig. 2 with the dotted lines in Fig. 3, reveal the importance of mutual coupling between the two continua. The further significance of this is discussed below.

Other generic properties of breakup effects emerge when we compare various characteristics of all the DPPs. The volume integrals of the real and imaginary parts of the DPPs are calculated by subtracting the volume integrals $J_{\rm R}$ and $J_{\rm I}$ of the real and imaginary parts of the bare potential, from those of the inverted potentials, to give $\Delta J_{\rm R}$ and $\Delta J_{\rm I}$ presented in Table I. The volume integrals are conventionally defined [1], with positive signs indicating

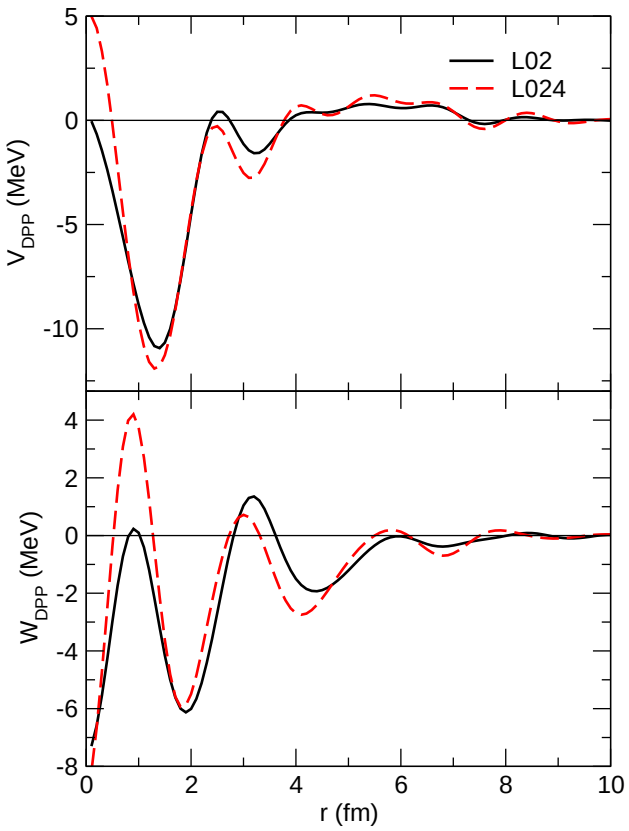

FIG. 2: For 30.0 MeV deuterons on ^{16}O, showing the real (upper panel) and imaginary (lower panel) DPPs for specific breakup couplings. The solid lines give the DPP for the L02 case, the dashed lines are for the L024 case.

attraction or absorption. Table I also presents: the changes in rms radii, $\Delta R_{\rm R}$(rms) and $\Delta R_{\rm I}$(rms), of the real and imaginary potentials; the change ΔCS in reaction cross section due to the coupling; the quantity $\rho_{\rm I}$ defined below; and the cross section to the breakup states, indicated as 'BU CS' in the tables. The value of $\Delta J_{\rm I}$ for the L02 case is much less than the sum of the values for the L0 and L2 cases, an effect of continuum-continuum coupling. It is generally accepted that the continuum-continuum coupling is important, but a comparison of the L0andL2 and L02 DPPs etc. in Table I shows the importance quantitatively.

For the L0, L2 and L0andL2 cases, there is an approximate proportionality between the change in reaction cross section and the change in the volume integral of the imaginary potential. The quantity $\rho_{\rm I} = \Delta{\rm CS}/\Delta J_{\rm I}$ presented in Table I is roughly the same for the L0 and L2 cases, but is distinctly less in the L02andL2, L02 and L024 cases.

Similar L02 and L024 breakup calculations have been carried out for deuterons on ^{39}Ca

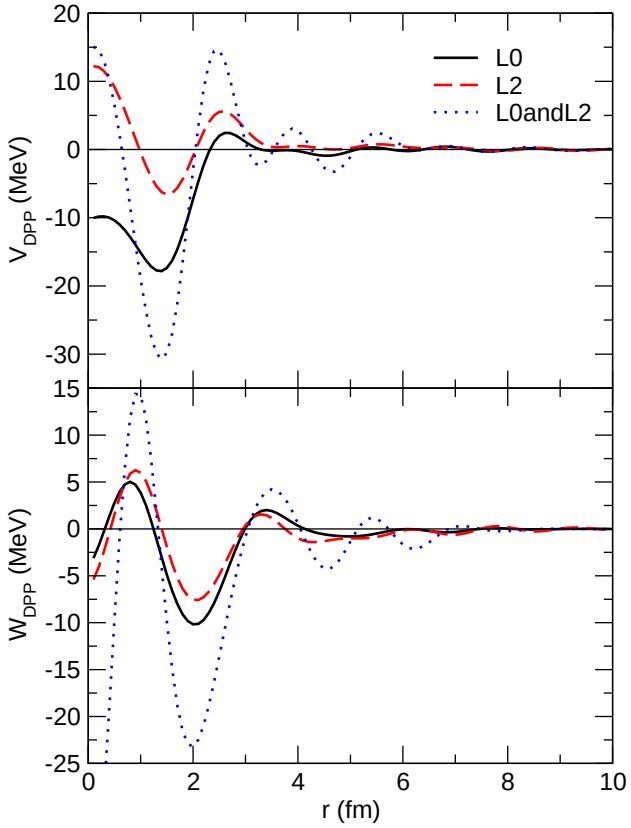

FIG. 3: For 30.0 MeV deuterons on ^{16}O, showing the real (upper panel) and imaginary (lower panel) DPPs for specific breakup couplings. The solid lines give the DPP for the L0 case, the dashed lines are for the L2 case and the dotted lines are for the L0andL2 case, as defined in the text.

and ^{40}Ca and quantities characterising the DPPs are given in Table II. As in the other cases, $L = 4$ coupling decreases ΔCS. In 9 of the 11 cases in Table I and Table II the increase in total reaction cross section, ΔCS, is less than the cross section to the breakup channels, 'BU CS' in the table. This indicates that the inhibition of other absorptive processes by breakup is quite a general property. Further indications of the generic nature of breakup effects can be found in Table III which presents the same characteristics for 56 MeV deuterons scattering from ^{58}Ni, see Ref. [17]. The magnitudes of $\Delta J_{\rm R}$ and $\Delta J_{\rm I}$ are less for the higher energy deuterons, but apart from that, the pattern of changes for the three cases in common is very similar to what is presented in Table I. For 56 MeV deuterons on ^{58}Ni, the same relationship holds between values of $\rho_{\rm I}$ for the L0, L2 and L02 cases as shown in Table I, although the magnitudes are different. Moreover, for both 30 MeV on ^{16}O and 56 MeV

TABLE I: For 30 MeV deuterons scattering from ^{16}O, characteristics of the DPP generated by the L0, L2, L02 and L024 couplings defined in the text. For case L0andL2 there is coupling to the L0 and L2 continuum states, but with no coupling between them. $\Delta J_{\rm R}$ and $\Delta J_{\rm I}$ are volume integrals of the real and imaginary DPPs in MeV fm^3; $\Delta R_{\rm R}$(rms) and $\Delta R_{\rm I}$(rms) are the changes in rms radius of the real and imaginary terms in fm; ΔCS is the change in reaction cross section due to breakup in mb and $\rho_{\rm I}$ is defined in the text. BU CS is the cross section to the breakup states in mb.

Coupling	$\Delta J_{\rm R}$	$\Delta R_{\rm R}$(rms)	$\Delta J_{\rm I}$	$\Delta R_{\rm I}$(rms)	ΔCS	$\rho_{\rm I}$	BU CS
L0	15.61	−0.0547	26.14	0.0196	67.2	2.571	63.36
L2	−24.89	−0.0735	35.25	0.1360	79.60	2.258	83.30
L0andL2	−14.31	−0.1205	68.34	0.0765	134.10	1.962	135.29
L02	−9.04	−0.1932	35.42	0.1190	69.60	1.965	83.32
L024	−11.55	−0.2320	38.11	0.1105	55.60	1.459	93.04

TABLE II: For deuterons scattering from ^{39}Ca or ^{40}Ca at indicated laboratory energies in MeV. All other quantities have the same meaning as elsewhere.

E (lab.)	Target	Coupling	$\Delta J_{\rm R}$	$\Delta R_{\rm R}$(rms)	$\Delta J_{\rm I}$	$\Delta R_{\rm I}$(rms)	ΔCS	$\rho_{\rm I}$	BU CS
26.92	^{39}Ca	L02	−12.74	−0.2050	30.23	0.1819	54.7	1.810	64.45
26.92	^{39}Ca	L024	−18.10	−0.2625	28.62	0.1324	26.2	0.915	71.74
30.0	^{40}Ca	L02	−15.35	−0.2396	25.69	0.2217	62.6	2.437	72.18
30.0	^{40}Ca	L024	−12.32	−0.2411	26.32	0.0835	34.9	1.325	78.35
52	^{40}Ca	L02	−3.31	−0.1413	25.82	0.1688	97.7	2.622	95.70
52	^{40}Ca	L024	−3.78	−0.1606	27.07	0.1410	82.5	3.048	91.64

on ^{58}Ni, for example, $\Delta J_{\rm R}$ is positive for L0 coupling, negative but larger in magnitude for L2 coupling and negative and smallest in magnitude for L02 coupling. One difference is that for L02 coupling, ΔCS > BU CS for 52 MeV deuterons on ^{40}Ca and also for 56 MeV deuterons on ^{58}Ni, but the opposite is true for the 30 MeV cases. It might be expected that the increase in reaction cross section would at least equal the breakup cross section, but this is only true for the L0 cases and the 52 MeV and 56 MeV case with L02 coupling. The effect

TABLE III: For 56 MeV deuterons scattering from ^{58}Ni, characteristics of the DPP generated by the L0, L2 and L02 couplings defined in the text. All other quantities have the same meaning as elsewhere.

Coupling	$\Delta J_{\rm R}$	$\Delta R_{\rm R}$(rms)	$\Delta J_{\rm I}$	$\Delta R_{\rm I}$(rms)	ΔCS	$\rho_{\rm I}$	BU CS
L0	4.77	−0.042	15.25	0.0643	90.4	5.92	84.65
L2	−6.24	−0.0628	15.06	0.2245	86.6	5.75	88.25
L02	−1.55	−0.141	18.29	0.1956	86.7	4.74	83.62

of breakup in reducing ΔCS below the breakup cross section is most apparent for the L024 cases at the lower energies. For breakup on ^{16}O this effect is significant: for L024 coupling the $L = 4$ breakup continuum reduces the reaction cross section and at the same time leads to the largest breakup cross section. Evidently, the coupling to the $L = 4$ continuum has reduced the absorption as measured by ΔCS although the magnitude of $\Delta J_{\rm I}$ shows that the coupling has increased the effective imaginary potential.

In all cases, both L02 and L024 (but not L0) breakup coupling reduce the real volume integral and increase the imaginary volume integral. In all cases breakup coupling reduces the rms radius of the real potential and increases the rms radius of the imaginary potential. This effect on the radial properties of the potential might be discernible in the systematic comparison of phenomenological deuteron potentials and folding model potentials.

In order to throw some light on these effects we have plotted the quantity $R(l)$ which can be calculated for the case of any particular breakup coupling:

$$R(l) = (2l + 1)(1 - |S_l|^2) - (2l + 1)(1 - |S_l|^2)_{\rm bare}. \quad (1)$$

The subscript 'bare' indicates the S_l is for the bare potential. $R(l)$ is a measure of the contribution for partial wave l to the change in reaction cross section induced by the coupling. In Fig. 4 a comparison of $R(l)$ for the L0, L2 and L02 cases shows that the extra absorption generated by breakup tends to be at higher l for L2 coupling than for L0 coupling. Comparison of $R(l)$ for the L2 and L02 cases shows that the coupling between the $L = 0$ and $L = 2$ continua reduces the contribution of breakup to the reaction cross section except at the largest l values. This is consistent with the ΔCS values in Table I. For all cases, breakup coupling actually decreases the reaction cross section for partial wave $l = 6$, a 'wrong way' effect as discussed in Ref. [27]. Fig. 5 shows that inclusion of BU to the $L = 4$ continuum

further reduces the partial wave reaction cross section for almost all partial waves, although this coupling does increase the breakup cross section.

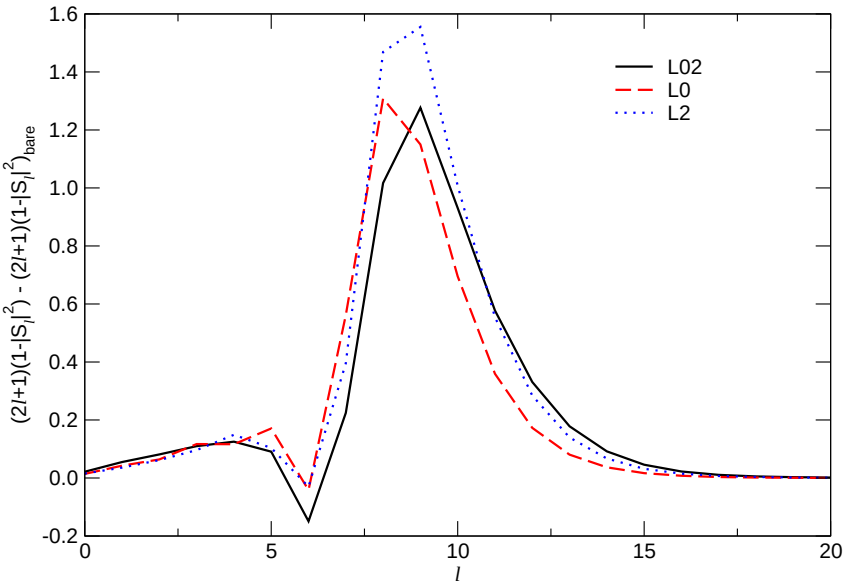

FIG. 4: For 30.0 MeV deuterons on ^{16}O, the quantity $R(l)$ defined in Eqn. 1 is plotted for the L0 (dashed), L2(dotted) and L02 (solid) breakup cases.

IV. FURTHER IMPLICATIONS OF THE BREAKUP CALCULATIONS

Apart from the characteristics of the DPPs, there are further implications to be drawn from the breakup calculations.

A. Evidence for dynamical non-locality

The L0andL2 case is of particular interest: There is no coupling between the L0 channels and the L2 channels and, as a consequence, the DPP generated by L0 coupling should add to the DPP generated by L2 coupling to give the DPP for L0andL2 coupling. This additivity rule applies to the underlying non-local DPPs; the formal argument is given in the Appendix. When, as here, the local equivalent potentials do not add to give the total local DPP, this is evidence for dynamical non-locality of the underlying DPPs. Examples have been presented

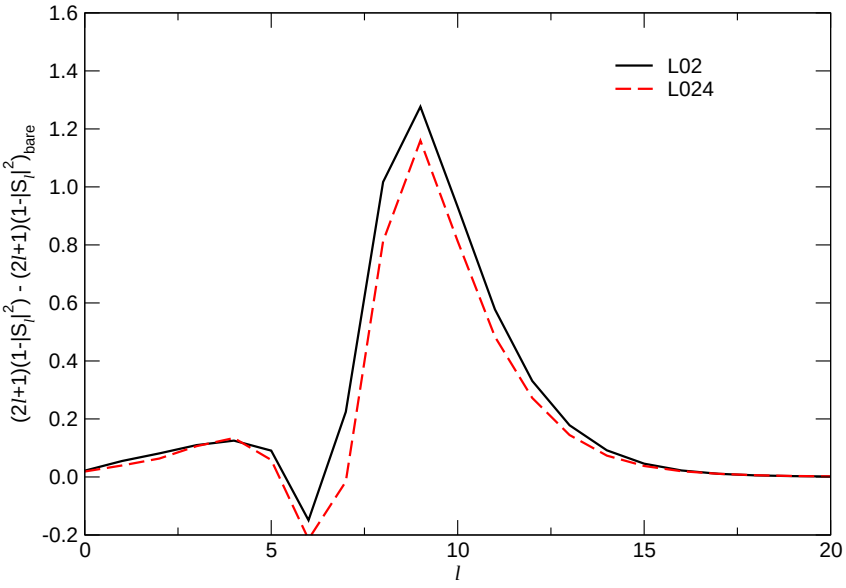

FIG. 5: For 30.0 MeV deuterons on ^{16}O, the quantity $R(l)$ defined in Eqn. 1 is plotted against l for the L02 (solid line) and L024(dashed line) cases. The partial wave reaction cross section is reduced, for almost all l, by the coupling to the $L = 4$ continuum, as also reflected in ΔCS.

in Refs. [28, 29] and in the first of these references a simple argument for the non-additivity of the local equivalents of non-local potentials was given.

From Table I we see that the sum of the $\Delta J_{\rm R}$ values for the L0 and L2 cases is -9.28 MeV fm^3 whereas it is -14.31 MeV fm^3 for the L0andL2 case in which there is no inter-continuum coupling. The corresponding figures for $\Delta J_{\rm I}$ values are 61.39 MeV fm^3 and 68.34 MeV fm^3, respectively. This is evident also from the point-by-point DPPs presented in Fig. 6 which compares the (local equivalent) DPP for the L0andL2 case with the sum of the local DPPs for the L0 and L2 cases. There is a substantial difference.

It will be noticed from Table I that the breakup cross section for the L0andL2 case, 135.29 mb, is not equal to the sum of the L0 and L2 breakup cross sections, 63.36 + 83.30 = 146.66 mb. In fact, in the L0andL2 case, the individual cross sections for the L0 and L2 channels are 56.16 mb and 79.13 mb, respectively. The L0 cross section, but not the L2 cross section, is modified by the coupling of the other channel to the elastic channel, in the absence of direct coupling. Because the elastic channel wave function is influenced by the sum of the DPPs,

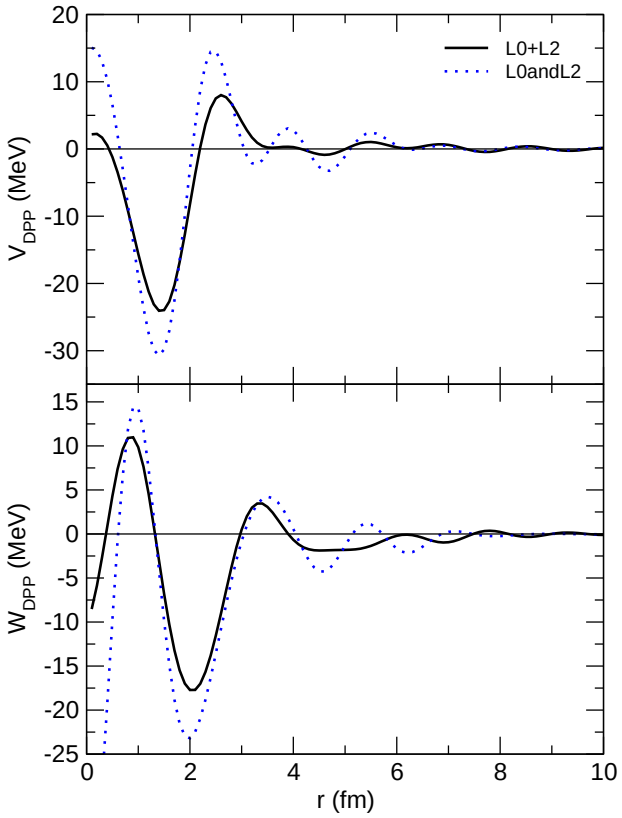

FIG. 6: For 30.0 MeV deuterons on ^{16}O, showing the real (upper panel) and imaginary (lower panel) DPPs for specific breakup couplings. The solid lines give the sum of the DPPs for the L0 and L2 cases, and the dotted lines give the DPP for the L0andL2 case.

this does not conflict with the fact that the non-local DPPs add. This indirect influence is an argument for comparing results using non-local and local equivalent distorting potentials in direct reactions. The Appendix gives a formal account of these effects.

B. Consequences of interactions between breakup continua

It is conspicuous that when the monopole and quadrupole excitation channels are inter-coupled, as in the L02 case, neither the total reaction cross section nor the breakup cross section increases much as a result. Indeed, ΔCS for the L02 case is less than for the L2 case. Can we explain why the additional inclusion of $L = 0$ breakup reduces the reaction cross section? A clue is one aspect of non-locality as follows: The behavior of $|S_l|$ for deuterons is intermediate between that for nucleons, for which $|S_l|$ does not become very small for

the lowest l, and the behavior for heavier particles. For the lowest values of l, $|S_l|$ becomes progressively smaller as the projectile mass increases see Ref. [30, 31] (^{6}Li and ^{7}Li being exceptions). For deuterons, the relatively large $|S_l|$ for low l is consistent with the results of the notch test and suggests that there is a substantial probability of a deuteron returning to its ground state after its encounter with the nucleus. The excitation out of its ground state, out of the elastic channel, and then back, is a non-local effect, see Austern [32]. The excitation of the deuteron from its ground state can be considered a temporary distortion and when monopole and quadrupole continua are coupled together, the total excitation of the pair is roughly the excitation of each alone. The two nucleons evidently penetrate the target nucleus more like free nucleons than like nucleons in a more tightly bound heavier projectile nucleus. It appears that the fragility of the deuteron actually facilitates its survival as it interacts with the nucleus, as suggested by Rawitscher long ago [33].

C. Further generic properties

In Section III regularities in the DPPs due to deuteron breakup were identified as generic, but they seem to apply to more general cases of projectile breakup. Certain characteristics of DPPs due to breakup have previously been identified as universal [34], occurring with the breakup of both ^{2}H and ^{6}Li projectiles. For deuterons, they apply for much heavier target nuclei than ^{16}O. In all cases the DPPs had strong undulations and the undulations in the imaginary DPP generally involve radial ranges where the DPP is emissive or nearly so. Also, in all cases L0 breakup generated weak surface attraction, and also attraction within the nucleus, whereas L02 breakup led to much stronger surface repulsion, with attraction within the nucleus, although the radial form is different for L0 breakup. These features appear in varying degrees in the DPPs found here. As further discussed in Section V, such undulations can be associated with l dependence, particularly when the coupling processes lead to substantially different effects for l less than or greater than the value for which $|S_l| \sim \frac{1}{2}$. The particularly strong contribution of low-l partial waves to the scattering of deuterons from ^{16}O, as revealed by a notch test, makes deuteron scattering from ^{16}O at 30 MeV susceptible to this effect.

V. TELP INVERSION: EVALUATION AND IMPLICATIONS

A. Evaluation of TELP inversion

The use of a weighted TELP inverted potential as the SRP for inversion, when using the Imago inversion code, has a useful by-product. That by-product is all the information required to determine the volume integrals and other characteristics of the DPP calculated from the TELP potential itself. These characteristics are presented in Table IV and can be compared with the same characteristics presented in Table I for DPPs calculated using exact S-matrix inversion. The differences are large, particularly for the L02 and L024 cases. In both cases $\Delta J_{\rm I}$ is higher while at the same time ΔCS is much lower. For all cases$|S_l|$ calculated from the weighted TELP is greater than that produced by the coupled channel code for all l greater than that from which $|S_l| \sim \frac{1}{2}$. This tends to reduce ΔCS. As a result, $\rho_{\rm I}$ is, for the L02 and L024 cases respectively, about a half and a third of the values for the S-matrix inverted potentials. This is consistent with the fact that $\Delta R_{\rm I}$(rms) is much too low for TELP potentials, suggesting that the imaginary potential is shifted inwards compared to the exact S-matrix inverted potential.

TABLE IV: For 30 MeV deuterons scattering from ^{16}O, characteristics of the DPP, generated by the L0, L2, L0andL2, L02 and L024 couplings defined in the text. These values relate to the potentials calculated by TELP inversion, and all other aspects of the Table are as for Table I.

Coupling	$\Delta J_{\rm R}$	$\Delta R_{\rm R}$(rms)	$\Delta J_{\rm I}$	$\Delta R_{\rm I}$(rms)	ΔCS	$\rho_{\rm I}$	BU CS
L0	6.05	−0.0684	19.74	−0.0230	43.80	2.219	63.36
L2	−9.99	−0.0903	42.40	0.0916	55.50	1.309	83.30
L0andL2	−3.63	−0.1618	61.65	0.0589	87.3	1.416	135.29
L02	−1.74	−0.1772	42.92	0.0375	39.20	0.913	83.32
L024	−4.47	−0.2016	42.11	0.0024	23.30	0.553	93.04

Some qualitative properties remain the same, e.g. $\Delta J_{\rm R}$ is positive for the L0 case and negative for the L2 case, but the magnitudes are very different. Therefore, conclusions from quantities such as those presented in Table I could not be reliably obtained from TELP potentials. The much lower values of ΔCS presented in Table IV would greatly exaggerate the relationship noted above between ΔCS and the cross section to breakup channels.

The elastic scattering angular distributions for the TELP inverted potentials differ considerably from the corresponding coupled channel elastic scattering angular distributionss, particularly at backward angles. For the L02 case at 150° the angular distribution corresponding to the TELP potential is a factor of 2 lower than the true value. The S-matrix inverted potentials always precisely reproduce the coupled channel elastic scattering angular distributions.

The TELP potentials reflect the non-additivity of the local equivalent DPPs in the L0andL2 case where the sums of $\Delta J_{\rm R}$, $\Delta J_{\rm I}$ and ΔCS in the L0 and L2 cases in Table IV are respectively -3.94 MeV fm^3, 62.14 MeV fm^3 and 99.30 mb compared with the values in the L0andL2 line.

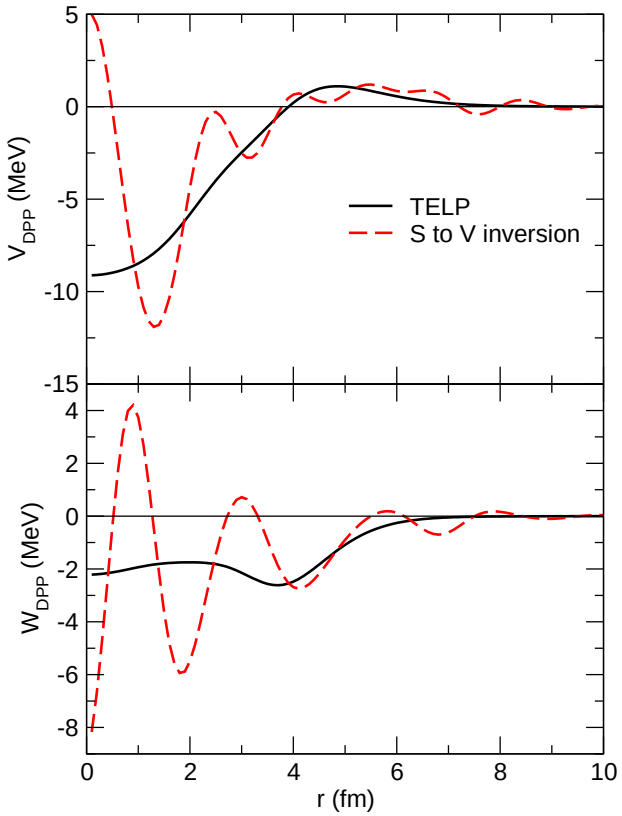

FIG. 7: For 30.0 MeV deuterons on ^{16}O, comparing the exact and TELP inverted potentials for the case with L024 coupling. The solid lines give the TELP potential and the dashed lines the exact S-matrix inverted potential. The real potential is in the upper panel and the imaginary part in the lower panel.

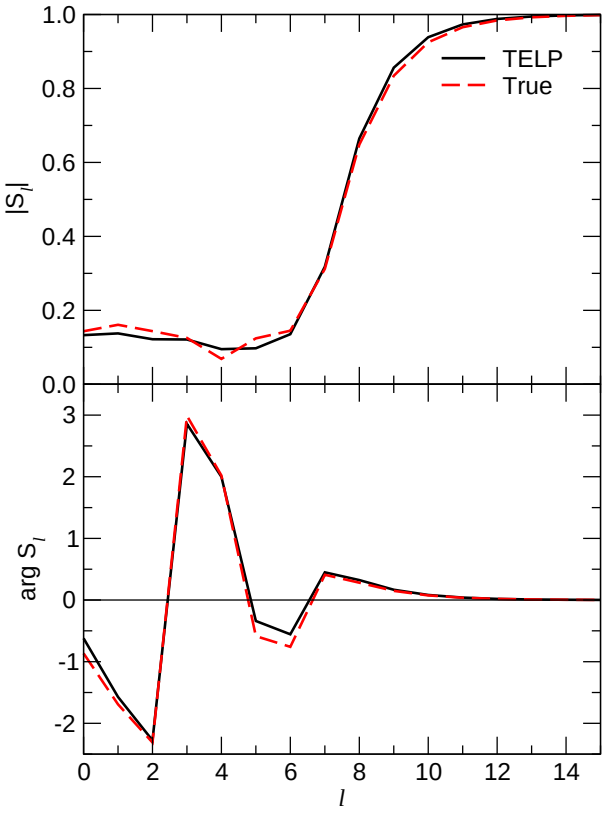

FIG. 8: For 30.0 MeV deuterons on ^{16}O, comparing the CDCC S_l with S_l calculated from the TELP, both for L024 coupling. The solid lines give the TELP values and the dashed lines the CDCC values, with $|S_l|$ in the upper panel and $\arg S_l$ in the lower panel.

B. Conclusions drawn from TELP potentials

The TELP inverted potentials are smooth and do not have the undularity, evident in Fig. 1, of the S-matrix inverted potentials. Figure 7 presents a direct comparison of the TELP and exact DPPs for the L024 case. Figure 8 compares S_l calculated from the TELP potential with that directly from the CDCC calculation. It reveals an alternation of the CDCC S_l about the TELP S_l: for example $|S_l|_{\rm CDCC} - |S_l|_{\rm TELP}$ is ≤ 0 for $l \geq 6$ and for $l = 4$ but $|S_l|_{\rm CDCC} - |S_l|_{\rm TELP} > 0$ for all other l. The deviations of the L0, L2 and L02 TELP potentials follow very similar patterns to that for the L024 TELP potential, shown in Fig. 8 (the L0 case has larger differences for low values of l).

The undularity of the S-matrix equivalent inverted potential appears to reflect the l-dependent difference of Fig. 8. Apart from $l = 4$, the difference in $|S_l|$ is between high and

low values of l; the difference in $\arg S_l$ varies in a similar way. For both L02 and L024 cases, the TELP $|S_l|$ is too large for high l and too low for low l. Recalling the $2l+1$ weighting factor, this accounts for the fact that the ΔCS values in Table IV are considerably less than the correct values in Table I, affecting the relationship with breakup cross section that was discussed above. In Ref. [35] it is shown how a small l-dependent factor applied to an l-independent S-matrix generates undulations in the corresponding inverted potential. Finally we remark that the undularity in the S-matrix inverted potentials, as seen in Figure 7, is not sporadic, but follows a consistent pattern in all examples of breakup effects that we have studied.

Although TELP inversion is imperfect, *qua* inversion, it has thrown light on the the l dependence of the deuteron OMP, and also provides a useful SRP for inversion in difficult cases.

VI. DISCUSSION AND CONCLUSIONS

The excitation of a deuteron as it interacts with a target nucleus generates a contribution to the deuteron-nucleus potential that is both non-local and l dependent. The conventional OMP that is employed to describe the elastic scattering of deuterons from nuclei is, however, both local and l independent. Such phenomenological local potentials are widely regarded as giving 'satisfactory' fits to elastic scattering data, although the requirement for precise fits results in potentials with unusual features, see for example Ref. [36]. Local potentials, often with globally fitted parameters, are widely used in the analysis of direct reactions involving deuterons leading to spectroscopic information. The primary goal of the present work, of which this paper presents the first part, is to gain an understanding of the consequences, for direct reactions, of the fact that a conventional OMP is the local equivalent of a potential that is actually nonlocal. We emphasise that the subject is dynamical non-locality, associated with the excitation of one of the interacting nuclei (the projectile, in this work), and not the non-locality arising from knock-on exchange processes which, for the particular case of (d,p) reactions, can be allowed for, see Ref. [5].

In order to determine the effects of dynamical non-locality for general direct reactions involving deuterons, we require the exact local equivalents to the non-local potentials generated by the breakup of the deuteron as it interacts with the target nucleus. The initial

motivation for the work reported in this paper was the determination of such local potentials. However, a number of findings have emerged that are of independent interest.

The interaction and breakup of 'fragile' nuclei is a subject with various aspects; for example, the effect of breakup on fusion processes has been exhaustively studied, for a recent review see Ref. [37]. The contribution of breakup to the departure from folding model systematics was an early motivation for CDCC studies which were mostly devoted to the effect on the interaction in the surface region. Nevertheless the study of the DPP arising from breakup coupling reveals a number of aspects of general significance. In particular, we note that in the case we study, notch tests reveal that the interest in the DPP is not confined to the surface region. For deuterons interacting with ^{16}O the coupling modifies the potential over almost the whole radial range, and in ways which are of intrinsic interest for the understanding of inter-nuclear interactions. The dynamically generated interaction is not smooth, and a comparison with earlier work suggests that there exist generic properties that apply widely to DPPs arising from coupling to breakup channels. Studying breakup effects in the context of deuteron scattering has the advantage that, considered as a cluster nucleus, its structure is unique, something that is not true of many other nuclei for which the effects of breakup processes have been studied, e.g. Ref. [38].

Among the facts that have emerged, some are not particularly surprising. An example is the fact that coupling to $L = 2$ breakup states contributes to $|S_l|$ for higher values of l than breakup to the $L = 0$ continuum. What might be unexpected is the fact that the inclusion of the $L = 4$ continuum *reduces* the absorption from the elastic channel, or the fact that the inclusion of $L = 0$ and $L = 2$ breakup together, with full mutual coupling, can make a smaller contribution to the total reaction cross section than $L = 2$ coupling alone.

The local equivalent potentials representing the DPPs have a pattern of undulations which indicates that the underlying DPP is l dependent as well as non-local. The undulations have general features similar to those found in breakup calculations for 56 MeV deuterons on ^{58}Ni, as well as for deuterons on ^{39}Ca and ^{40}Ca over a range of energies. It is also found that breakup coupling systematically reduces the rms radius of the real part of the potential and increases the rms radius of the imaginary part, compared to the bare folding model potential. These apparently generic properties could be studied with precision elastic scattering experiments together with precision model-independent fitting. How much these effects would survive the inclusion of other reaction processes, such as coupling to mass-

1 and mass-3 channels, remains for future studies, as does the full representation of spin effects. The undulatory potentials can not represent an l-independent potential since such a potential $V(r)$ must have a zero derivative at $r = 0$ since otherwise the potential as a function in 3 dimensions would have a cusp at the nuclear center.

The occurrence of undulations deserves experimental study. In cases such as that reported in Ref. [36], where precise, wide angular range data are fitted exactly using model independent methods, such features do appear. It is likely that if more precise wide range data were fitted to the same standard that is normal for electron scattering analyses, then such features would commonly be found. This could then provide an indirect method of exploring the possible l-dependence of the nuclear OMP. The systematic undulatory properties of the local potentials are consistent with previous CC plus inversion results, and are more indirectly supported by the results of model independent fitting [36]. Undularity cannot be ignored and should be considered seriously as a property of the deuteron-nucleus potential.

The CDCC calculations presented an opportunity to evaluate the weighted TELP procedure for inversion. We find that for the present case it would not provide a reliable method for studying the properties of the DPP. The l-dependent differences between S_l direct from the CDCC calculation and S_l from the TELP potential suggest why the inverted potential is undulatory, and also why the TELP reaction cross section is incorrect. This can be seen from the Δ CS values in Table IV which are too low.

The local potentials derived here are applied in a subsequent paper, Ref. [10], to the study of the effect of dynamical non-locality on transfer reactions. However, the present work has already shown, through the non-additivity of local equivalent DPPs, that breakup coupling leads to appreciable non-local effects.

VII. APPENDIX: ADDING NON-LOCAL DPPS

We present a simplified model demonstration that formal non-local DPPs arising from coupling to channels that are coupled to the elastic channel but not to each other add to give the total non-local DPP. We consider a spinless projectile on a spinless target so the total conserved angular momentum is the orbital angular momentum. The orbital angular momentum operator is implicit in the kinetic energy operator T in the coupled channel equations, with channel 0 the elastic channel. We first consider the example of two spinless

states:

$$(T + V_{00}(r) - E_0)\psi_0(r) = -V_{01}(r)\psi_1(r) - V_{02}(r)\psi_2(r), \tag{2}$$

$$(T + V_{11}(r) - E_1)\psi_1(r) = -V_{10}(r)\psi_0(r) - V_{12}(r)\psi_2(r), \tag{3}$$

$$(T + V_{22}(r) - E_2)\psi_2(r) = -V_{20}(r)\psi_0(r) - V_{21}(r)\psi_1(r). \tag{4}$$

If there is no coupling between channels 1 and 2, Eqs 3 and 4 become Eqs 5 and 6:

$$(T + V_{11}(r) - E_1)\psi_1(r) = -V_{10}(r)\psi_0(r), \tag{5}$$

$$(T + V_{22}(r) - E_2)\psi_2(r) = -V_{20}(r)\psi_0(r). \tag{6}$$

We can rewrite the last two equations, defining G_1 and G_2 as:

$$\psi_1 = \frac{1}{E_1^+ - T - V_{11}} V_{10}\psi_0 \equiv G_1 V_{10}\psi_0 \tag{7}$$

and

$$\psi_2 = \frac{1}{E_2^+ - T - V_{22}} V_{20}\psi_0 \equiv G_2 V_{20}\psi_0. \tag{8}$$

The equation for the elastic channel wave function ψ_0 is therefore

$$(T + V_{00}(r) - E_0)\psi_0(r) = -V_{01}G_1V_{10}\psi_0 - V_{02}G_2V_{20}\psi_0 \tag{9}$$

so the effective elastic channel potential is

$$V_{00} + V_{01}G_1V_{10} + V_{02}G_2V_{20} \equiv V_{00} + \mathrm{DPP}_1 + \mathrm{DPP}_2. \tag{10}$$

which is to say that the (non-local and l-dependent) DPPs due to the coupling to channel 1 and to channel 2 add to give the total (non-local and l-dependent) DPP. Note, however, that ψ_1 is affected by the coupling in channel 2 through the effect on the elastic channel ψ_0 so that the inelastic cross sections in each of channel 1 and channel 2 may be strongly dependent on the coupling in the other channel.

The important point here is that although the total DPP is the sum of the DPPs separately due to the excitations in channels 1 and 2, the local and l-independent representation

of this DPP, i.e. the local potential that gives in a single channel calculation the same ψ_0 in the asymptotic region, and hence the same elastic S-matrix S_l, as the coupled equations, will certainly not be a sum of the local representations of DPP_1 and DPP_2. The local equivalent of the sum of two non-local potentials is not the sum of the local equivalents of each potential, see Ref. [28].

It is straightforward to see that the above all holds when equations 5 and 6 become sets of coupled equations with no coupling between each set:

$$(T + V_{ii} - E_i)\psi_i = -\sum_j V_{ij}\psi_j - V_{i0}\psi_0 \tag{11}$$

$$(T + V_{mm} - E_m)\psi_m = -\sum_n V_{mn}\psi_n - V_{m0}\psi_0 \tag{12}$$

in which case Eqn. 2 becomes

$$(T + V_{00}(r) - E_0)\psi_0(r) = -\sum_i V_{0i}(r)\psi_i(r) - \sum_m V_{0m}(r)\psi_m(r). \tag{13}$$

The formal (vector) solution to Eqn. 11 can be written in terms of the coupled Green function for

$$(T + V_{ii} - E_i)\psi_i + \sum_j V_{ij}\psi_j = 0 \tag{14}$$

i.e.

$$G_{ij} \equiv \frac{1}{E^+ - H_{ij}} \tag{15}$$

so again we get the total potential:

$$V_{00} + \sum_{ij} V_{0i}G_{ij}V_{j0} + \sum_{mn} V_{0m}G_{mn}V_{n0}. \tag{16}$$

Thus, the non-local DPP arising from the coupling of the elastic channel to a set of channels $i, j, \ldots$, which are coupled together, adds to the non-local DPP arising from coupling of the elastic channel to a set of channels $m, n, \ldots$ to give the total non-local DPP providing there is no coupling between the channels $i, j, \ldots$ and the channels $m, n, \ldots$. But, there is no reason to suppose that the local equivalents add in the same way to give the total local equivalent DPP.

The local DPPs are far from being additive in the present deuteron breakup cases, and this can be taken as an indication of the dynamical non-locality of the separate DPPs. Again, although the coupling in one set of channels has no influence on the (non-local, l-dependent)

DPP arising from the other set of channels, coupling in each set *does* affect inelastic cross sections in the alternate set of channels.

In some circumstances the local equivalent DPPs do add quite closely to give the total local DPP, and the comparison might be informative. A case where the local equivalent DPPs do add very closely is that of 80 MeV ^{16}O scattering from ^{208}Pb [39]. There were two classes of local DPPs: (i) due to inelastic excitation, and, (ii) due to particle transfer. There was no mutual coupling between the collective and transfer processes. That case differs from the present deuteron case in a number of respects: the projectile wavelength is much shorter, and the coupling, and hence the DPPs, are confined to the surface region. In addition, the bare potential was almost purely real in the active radial range which is probably why the real DPPs were predominantly attractive in the surface region, unlike the deuteron breakup DPPs.

VIII. ACKNOWLEDGMENT

The authors are very grateful to Ian Thompson for modifications of his powerful FRESCO code enabling the L0andL2 calculations.

[1] G.R. Satchler, *Direct Nuclear Reactions* (Clarendon Press, Oxford, 1983).

[2] N. Keeley and R.S. Mackintosh, Phys. Rev. **C 90**, 044602 (2014).

[3] R.C. Johnson and P.J.R. Soper, Phys. Rev. **C 1**, 976 (1970).

[4] R.C. Johnson and P.C. Tandy, Nucl. Phys. A**235**, 56, (1974).

[5] L.J. Titus, F.M. Nunes, and G. Potel, Phys. Rev. **C 93**, 014604 (2016).

[6] R.S. Mackintosh, A.A. Ioannides, and S.G. Cooper, Nucl. Phys. **A483**, 173 (1988).

[7] S.G. Cooper and R.S. Mackintosh, Nucl. Phys. **A511**, 29 (1990).

[8] G.H. Rawitscher, Nucl. Phys. A **475**, 519 (1987).

[9] I.J. Thompson, Comput. Phys. Rep. **7**, 167 (1988).

[10] N. Keeley and R.S. Mackintosh, in preparation.

[11] G.H. Rawitscher, Phys. Rev. **C9**, 2210 (1974).

[12] J.P.Farrell Jr, C.M. Vincent, and N. Austern, Ann. Phys. (NY), **96**, 333 (1976).

[13] M. Yahiro, N. Nakano. Y.Iseri, and M. Kamimura, Prog. Theor. Phys. **67**, 1467 (1982).

[14] N. Austern, Y. Iseri, M. Kamimura, M. Kawai, G. Rawitscher, and Y. Yahiro, Physics Reports **154**, 125 (1987).

[15] Y. Sakuragi, M. Yahiro and M. Kamimura, Prog. Theor. Phys. Supp. 89, 136 (1986).

[16] R.S. Mackintosh and A.M. Kobos, Phys. Lett. **B 116**, 95 (1982).

[17] R.S. Mackintosh and D.Y. Pang, Phys. Rev. **C86**, 047602 (2012).

[18] G. H. Rawitscher and S. N. Mukherjee, Nucl. Phys. A **342**, 90 (1980).

[19] A. J. Koning and J. P. Delaroche, Nucl. Phys. **A713**, 231 (2003).

[20] S.G. Cooper and R.S. Mackintosh, Inverse Problems, **5** (1989) 707.

[21] V.I. Kukulin and R.S. Mackintosh, J. Phys. G: Nucl. Part. Phys, **30**, R1 (2004).

[22] R.S. Mackintosh, arXiv:1205.0468.

[23] R.S. Mackintosh, Scholarpedia, 7(11):12032, (2012). doi:10.4249/scholarpedia.12032.

[24] M.A. Franey and P.J. Ellis, Phys. Rev. **C23**, 787 (1981).

[25] I.J. Thompson, M.A. Nagarajan, J.S. Lilley, and M.J. Smithson, Nucl. Phys. A **505**, 84 (1989).

[26] D.Y. Pang and R.S. Mackintosh, Phys. Rev. **C84**, 064611 (2011).

[27] R.S. Mackintosh, Phys. Rev. **C 88**, 054603 (2013).

[28] R.S. Mackintosh and N. Keeley, Phys. Rev. **C 81**, 034612 (2010).

[29] N. Keeley and R.S. Mackintosh, Phys. Rev. **C 83**, 044608 (2011).

[30] J. Cook, J.M. Barnwell, N.M. Clarke, and R.J. Griffiths, J. Phys. G: Nucl. Part. Phys, **6**, 1251 (1980).

[31] Ref. [1], p. 401.

[32] N. Austern, Phys. Rev. B **137**, 752 (1965).

[33] G.H. Rawitscher, Phys. Rev. **163**, 1223 (1967).

[34] A.A. Ioannides and R.S. Mackintosh, Phys. Lett. **B 169**, 113 (1986).

[35] R.S. Mackintosh, arXiv:1302.1097v3.

[36] M. Ermer, H. Clement, P. Grabmayr, G.J. Wagner, L. Friedrich, and E. Huttel, Phys. Lett. B**188**, 17 (1987).

[37] L.F. Canto, P.R.S. Gomes, R. Donangelo, J. Lubian, and M.S. Hussain, Physics Reports, **596**, 1 (2015).

[38] N. Keeley, R.S. Mackintosh, and C. Beck, Nucl. Phys. A **834**, 792c (2010).

[39] A.A. Ioannides and R.S. Mackintosh, Phys. Lett. **B 161**, 43 (1985).